

Hexagonal boron nitride thick film grown on a sapphire substrate via low-pressure chemical vapor deposition

Zhifu Zhu <sup>1,2</sup>, Zhongming Zhang <sup>3</sup>, Shaotang Wang <sup>2</sup>, Jijun Zou<sup>2\*</sup>, Yong Gan <sup>1</sup>, Ruibin Yang <sup>1</sup>, Yang Zhang <sup>1</sup>, Bingxu Long <sup>2</sup>

1. School of Information Engineering, Zhengzhou University of Technology, Zhengzhou, 450044, China

2. Engineering Research Center of Nuclear Technology Application (East China University of Technology), Ministry of Education, Nanchang, 330013, China

3. Engineering department, Lancaster University, Lancaster, LA14YW, United Kingdom

\*Corresponding author. E-mail: [jjzou@ecit.cn](mailto:jjzou@ecit.cn)

**Abstract:**

hexagonal boron nitride (h-BN) with a certain thickness has wide applications in semiconductor electronic devices. In this study, the relationship between the amount of ammonia borane and the thickness of h-BN films was investigated via low-pressure chemical vapor deposition (LPCVD) on a non-catalytic c-plane Al<sub>2</sub>O<sub>3</sub> substrate. Through various characterization methods, the grown film was confirmed to be h-BN. The effect of precursor concentration on the growth thickness of the h-BN film was studied, and it was found that the precursor concentration significantly affected the growth rate of the h-BN film. The results from SEM show that the amount of ammonia borane is 2000 mg, and a 1.295- $\mu$ m h-BN film is obtained. It will provide an experimental reference for the growth of thicker h-BN materials to prepare high-efficiency neutron detectors for radiation detection.

**Keywords:** Ammonia borane, Hexagonal boron nitride, LPCVD, Dehydrogenation

## 1. Introduction

h-BN is an important group III-V bandgap compound semiconductor material that is expected to find applications in high-power electronics, high-temperature high-radiation detection, and deep-ultraviolet detection due to its excellent properties such as high thermal conductivity, high resistivity, low dielectric constant, and high breakdown electric field [1-3]. And there are almost no dangling bonds on the surface of h-BN, which results in the least impact on electron transmission; therefore, it is an excellent candidate as substrate material for two-dimensional (2D) electronic products [4, 5]. Among the electronic device applications of h-BN, the most promising application is in the field of nuclear radiation detection due to the relatively high thermal neutron capture cross section ( $\sim 3840\text{b}$ ) of  $^{10}\text{B}$  in h-BN and the fact that neutron capture, charge collection, and electrical signal generation are all done within the detector body. If the isotope  $h\text{-}^{10}\text{BN}$  is used, it will be one of the most promising potential future semiconductor neutron-detecting materials to replace  $^3\text{He}$  gas neutron detectors. Current methods for h-BN film preparation mainly include mechanical stripping [6], liquid phase stripping [7], chemical vapor deposition (CVD) [8–11], and physical vapor deposition [12,13]. It is worth mentioning that the CVD method has unique advantages and potential for thin film growth, due to simple equipment, ease of operation, and low cost. The basis of the CVD method for synthesizing BN films is the decomposition of compounds containing B and N followed by their reaction on a substrate. Gaseous precursors (for example,  $\text{BF}_3/\text{NH}_3$ ,  $\text{BCl}_3/\text{NH}_3$ , and  $\text{B}_2\text{H}_6/\text{NH}_3$ ) and liquid precursors (e.g. trichloroborazine and borazine) for the growth of BN films are flammable, toxic, or contain decomposition products. Toxicity makes growth operations more difficult, resulting in potential safety hazards. Another CVD technique for growing h-BN is to use an ammonia borane with properties such as non-toxic, non-flammable, non-explosive, and easy to store at room temperature as a precursor reactant. When it undergoes a chemical reaction at high temperature, the reaction product is deposited on the substrate to complete the growth of h-BN. It has a B/N stoichiometric ratio of 1:1, and more importantly, it has a low decomposition temperature and produces no decomposition product pollution. As a boron source, it can also be used as a nitrogen source, a single precursor. Compared to other precursors, ammonia borane has a lower equilibrium vapor pressure, making it the most suitable choice for the growth of high-quality and highly controllable thin films [14]. The growth of h-BN films via CVD is mainly divided into two categories: the first condition is the growth of 2D materials (thin h-BN film with the thickness of a single layer or several atomic layers), and the other situation is thick film growth, which is used to prepare optoelectronic devices or semiconductor devices. Many researchers have synthesized h-BN films on Cu [15], Ni [16], Co [17], Pt [18], and other catalytic substrates using CVD. However, this method is only suitable for growing single-layer or few-layer h-BN films on catalytic substrates; When separated from the catalytic substrate, the film cannot continue to grow, which is limited in large-scale semiconductor electronic device applications.

In order to realize wafer-level h-BN for semiconductor electronic devices, it is necessary to consider the growth of thick film h-BN. Although Chen et al. grew h-BN with a thickness of only 228 nm on a sapphire substrate via LPCVD using ammonia borane, this was not a high-quality h-BN film but a deposition of snowflake like BNH polymer [19]. The h-BN with greater than 1  $\mu\text{m}$  thickness has not been reported in the literature.

In view of the current need for thick film h-BN applications, this study uses ammonia borane ( $\text{NH}_3\text{-BH}_3$ ) as a precursor, discusses the relationship between the amount of ammonia borane source and the thickness of h-BN growth, and analyzes the characteristics of h-BN grown under different

ammonia boranes. In this work, h-BN films with a thickness of 1.295  $\mu\text{m}$  were grown on a non-catalytic sapphire substrate via LPCVD using ammonia borane as a precursor. No peeling or cracking was observed on the surface of the h-BN films due to the nitriding treatment of the sapphire substrate for about 1 h prior to the film growth. This provides experimental support for the application of neutron detection or thick film semiconductor electronic devices.

## 2. Experimental process

This experiment used the LPCVD method to synthesize h-BN film, as shown in Figure 1. The precursor ammonia borane was heated using an independent heater, and the product after thermal decomposition of the ammonia borane, with Ar as the carrier gas, was passed into the dual-temperature zone high-temperature tube furnace to process h-BN film growth.

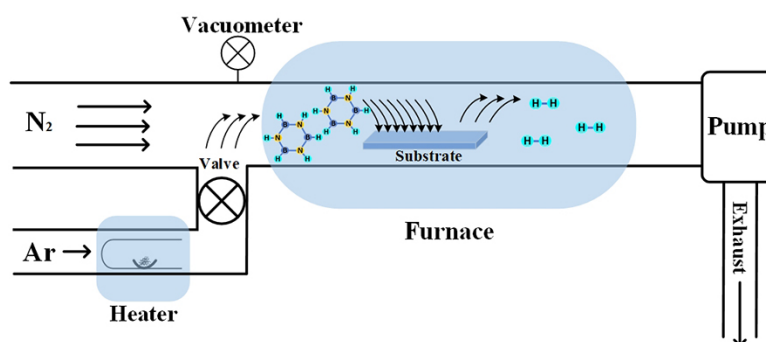


Figure 1 LPCVD system

The substrate used in the experiment was  $1 \times 1 \text{ cm}^2$  c-plane (0001)  $\text{Al}_2\text{O}_3$ . First, the substrate was placed in an ultrasonic cleaning machine and ultrasonically cleaned with acetone, absolute ethanol, and deionized water for 10 min. Then, the  $\text{Al}_2\text{O}_3$  was taken out after drying with nitrogen, placed in a sample boat, and sent to the tube furnace. The tube furnace was evacuated to below 1 Pa to remove air and heated to 1250  $^\circ\text{C}$  with passing  $\text{N}_2$  (80 sccm). Subsequently, the substrate is nitrided at this temperature for 1 h in order to form a thin amorphous  $\text{Al}_x\text{N}_y$  buffer layer on its surface and to reduce the mismatch between the substrate and the h-BN. A certain amount of ammonia borane was placed into an independent box furnace and heated for 5 min to 120  $^\circ\text{C}$ . 20 sccm Ar was used as the carrier gas to pass the ammonia borane decomposition product into the tube furnace for growth.  $\text{N}_2$  was introduced simultaneously, and the growth pressure was maintained at 500 Pa. After growth, the temperature of the tube furnace was lowered to room temperature under an  $\text{N}_2$  gas flow rate of 50 sccm. Finally, the sample was removed.

The high-temperature dehydrogenation of ammonia borane to form a BN film can be roughly divided into three steps [19], as shown in Figure 2. (1) Ammonia borane is decomposed into hydrogen, borazine, and polyaminoborane (80 ~ 180  $^\circ\text{C}$ ); (2) borazine and polyaminoborane are transported by the carrier gas to the substrate surface at a high temperature for further dehydrogenation to form polyiminoborane (130 ~ 700  $^\circ\text{C}$ ); (3) polyiminoborane is further dehydrogenated at high temperatures to form a BN film (1170 ~ 1500  $^\circ\text{C}$ ).

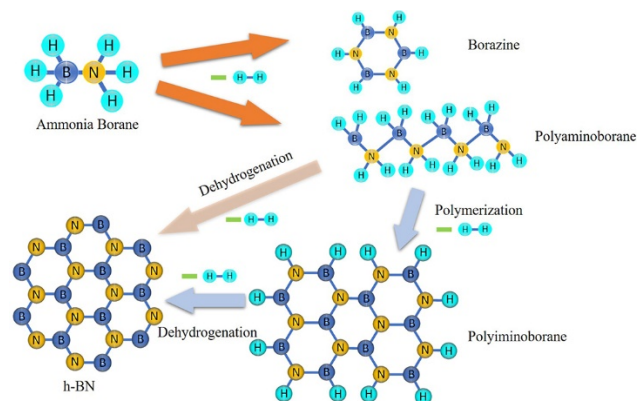


Figure 2 Schematic diagram of structural development from the dissociation of borazane to h-BN.

The surface morphology and thickness of the h-BN film were characterized by scanning electron microscopy (SEM, Zeiss Merlin Compact). Elemental composition and quantitative analysis of the film were performed using X-ray electron energy spectroscopy (XPS, Thermo Scientific Escalab 250Xi). The crystal structure, composition, and chemical composition of the film were characterized using X-ray diffraction (XRD, Bruker D2 PHASER), and Raman spectroscopy (Thermo Scientific DXR2) was used to characterize the crystallinity of the synthesized h-BN film. Transmission electron microscopy (TEM, JEM-2100-plus) was also used to characterize and analyze the microscopic crystal structure of the h-BN film.

### 3. Results and discussion

A high-temperature tube furnace was used to grow the BN film to clarify the relationship between precursor concentration and growth rate. The growth pressure was maintained at 500 Pa by adjusting the flow rate of N<sub>2</sub> using Ar with a flow rate of 20 sccm as the carrier gas. The ammonia borane precursor concentrations were 100, 500, 1000, 1500, and 2000 mg, which were grown for 120 min to obtain five samples.

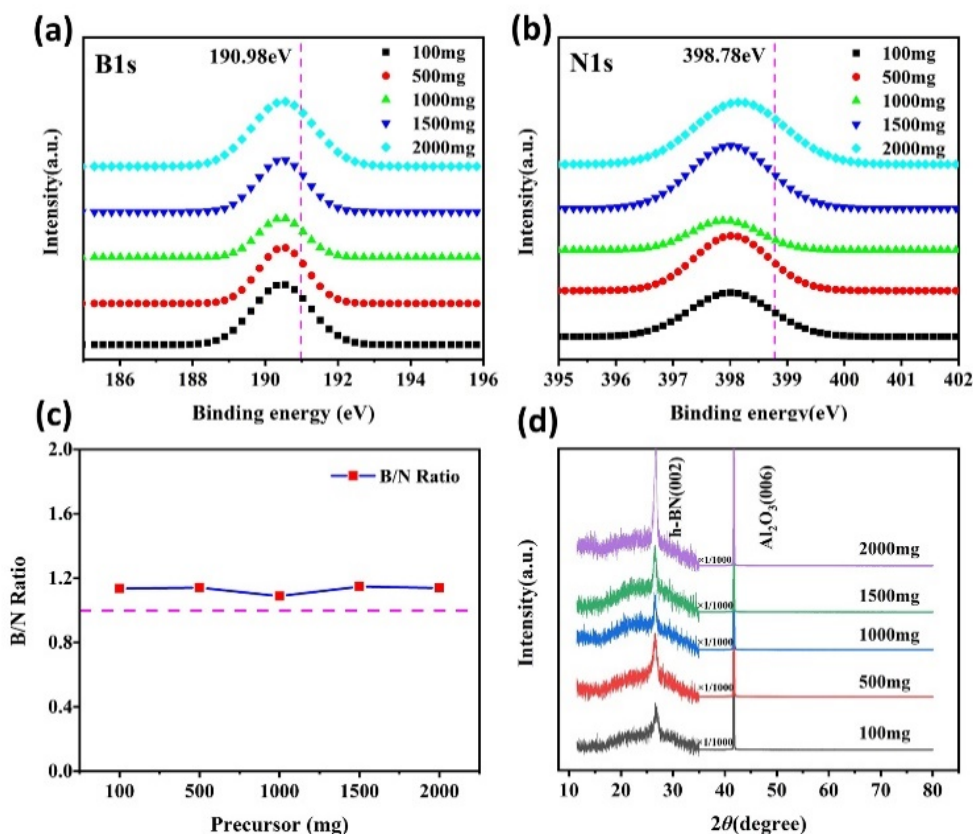


Figure 3 (a) XPS B1s spectra of the film samples. (b) XPS N1s spectra of the film samples. (c) Relationship between precursor concentration and the B/N ratio. (d) XRD  $\theta$ - $2\theta$  scan patterns.

At first, the influence of precursor concentration on the chemical state of the BN film was studied by XPS. As shown in Figures 3 (a) and 3 (b), peaks in the binding energies of B and N were found in the samples. While the B and N binding energies of the five samples lay between 190.4 and 190.5 eV and 398.1 and 398.3 eV, respectively, which correspond to the B–N bond [错误!未找到引用源。](#), there was no apparent difference in the chemical state observed, which may indicate that the precursor concentration had little effect on the chemical state of the film. In addition, the energy peaks of the B and N elements of the five samples were slightly lower than the 190.98 eV and 398.78 eV of the single-crystal h-BN film, respectively. According to a previous report by Kim et al. [20], the thermal decomposition of  $\text{NH}_3\text{-BH}_3$  consists of three steps. Therefore, the degree of dehydrogenation of  $\text{NH}_3\text{-BH}_3$  is related to the pyrolysis temperature and time. Incomplete dehydrogenation at lower growth temperatures leads to residual H atoms and the formation of a small amount of BNH polymer, and the binding energy shifts -towards the low-energy region. We analyzed atomic percentages in the film samples using the XPS results. The results are shown in Figure 3 (c). The B/N ratio of the five samples was close to 1:1, which indicates that B and N in the grown film mainly existed as B–N chemical bonds [21].

In addition, the crystal structure of the grown film was further characterized using XRD. As shown in Figure 3 (d), the diffraction peak at  $41.683^\circ$  originated from (006) crystal plane diffraction of the  $\text{Al}_2\text{O}_3$  substrate (pdf#10-0173), and the diffraction peak at approximately  $26.72^\circ$  [23] originated from (002) crystal plane diffraction of h-BN (pdf#34-0421). This indicates that the synthesized film was h-BN, and the diffraction peak intensity of the five samples was relatively high near  $26.5^\circ$ , suggesting that the amount of ammonia borane had no effect on the crystal quality of

the h-BN film.

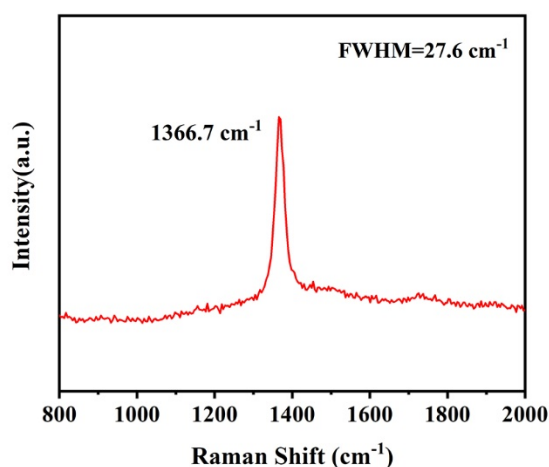


Figure 4 Raman spectrum of the grown h-BN film

Figure 4 shows a typical Raman spectrum of the h-BN film. In the low-frequency region, the clear dominant peak exhibited by the film at approximately  $1367\text{ cm}^{-1}$  was attributed to the B–N vibration mode ( $E_{2g}$ ) in the h-BN layer. The Raman spectrum further confirmed the successful growth of high-quality h-BN film with a hexagonal structure.

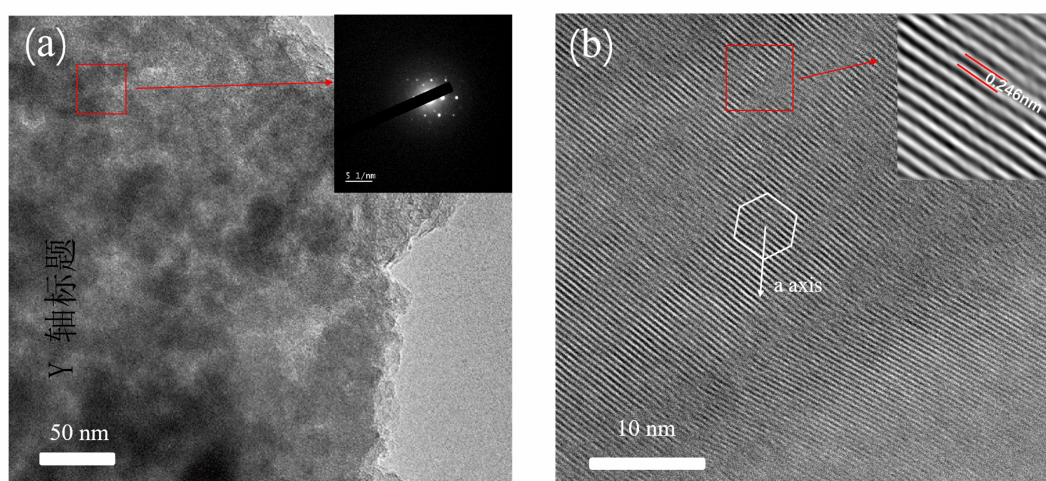


Figure 5 (a) TEM image of the BN film. The insert of (a) is the corresponding SEAD of the region. (b) Atomic image of the h-BN film. The insert of (b) is a further enlarged TEM image of the region.

Some h-BN thin films were gently scraped from the grown samples and placed on the carbon film to prepare TEM samples with a copper mesh. The samples were characterized using TEM. As shown in Figure 5 (a), the BN in bright field image can be visualized and the inset shows the corresponding SAED pattern. Six-fold symmetric diffraction spot was observed. Thus, from this inset, six spots of the hexagon correspond to h-BN ( $a_{\text{h-BN}}=2.5\text{ \AA}$ ). Then, the atomic structure of the film was studied and further expanded to obtain the microstructure of the film. As shown in Figure 5 (b), the crystallinity of the film was still better. The a-axis direction of the film is shown in Figure 5 (b). And from the HRTEM image calculated the lattice constant was  $2.46\text{ \AA}$ , consistent with the  $2.504\text{ \AA}$  of bulk h-BN [24]. It is further confirmed that the grown thin film was h-BN [24].

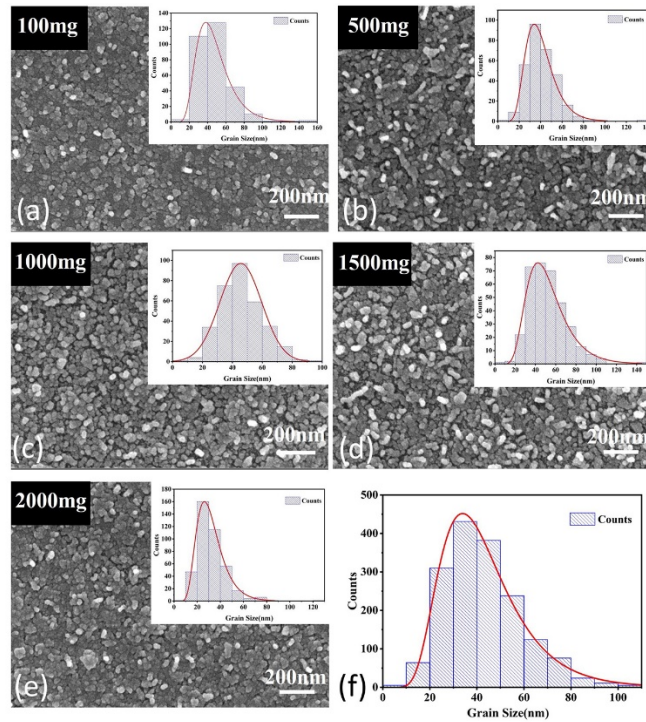


Figure 6 (a–e) Surface morphology of the BN film samples grown with different concentrations of ammonia borane. The inset is a statistic graph of grain size. (f) Statistical diagram of the surface grain size of all samples.

The surface morphology and thickness of the film were observed using SEM. From Figure 6 (a–e), we can see that the surface morphologies of the samples were basically the same, which proves that the surface roughness of the film was independent of the precursor concentration. Moreover, the grain size of the film is also observed in the SEM image. As shown in the inset on the left of Figure 6 (f), the typical grain size was about 30 ~ 50 nm and relatively dense. The nucleation density of the film may be high under a growth pressure of 500 Pa, contributing to small and dense grains. The growth of h-BN thin films synthesized via LPCVD may follow an island growth model rather than a layer-by-layer growth model, which is mainly formed by the accumulation of homogeneous nucleation to produce a thin film. So, the particle aggregation in the films can be clearly discovered from the SEM results (Figure 6 (a–e)).

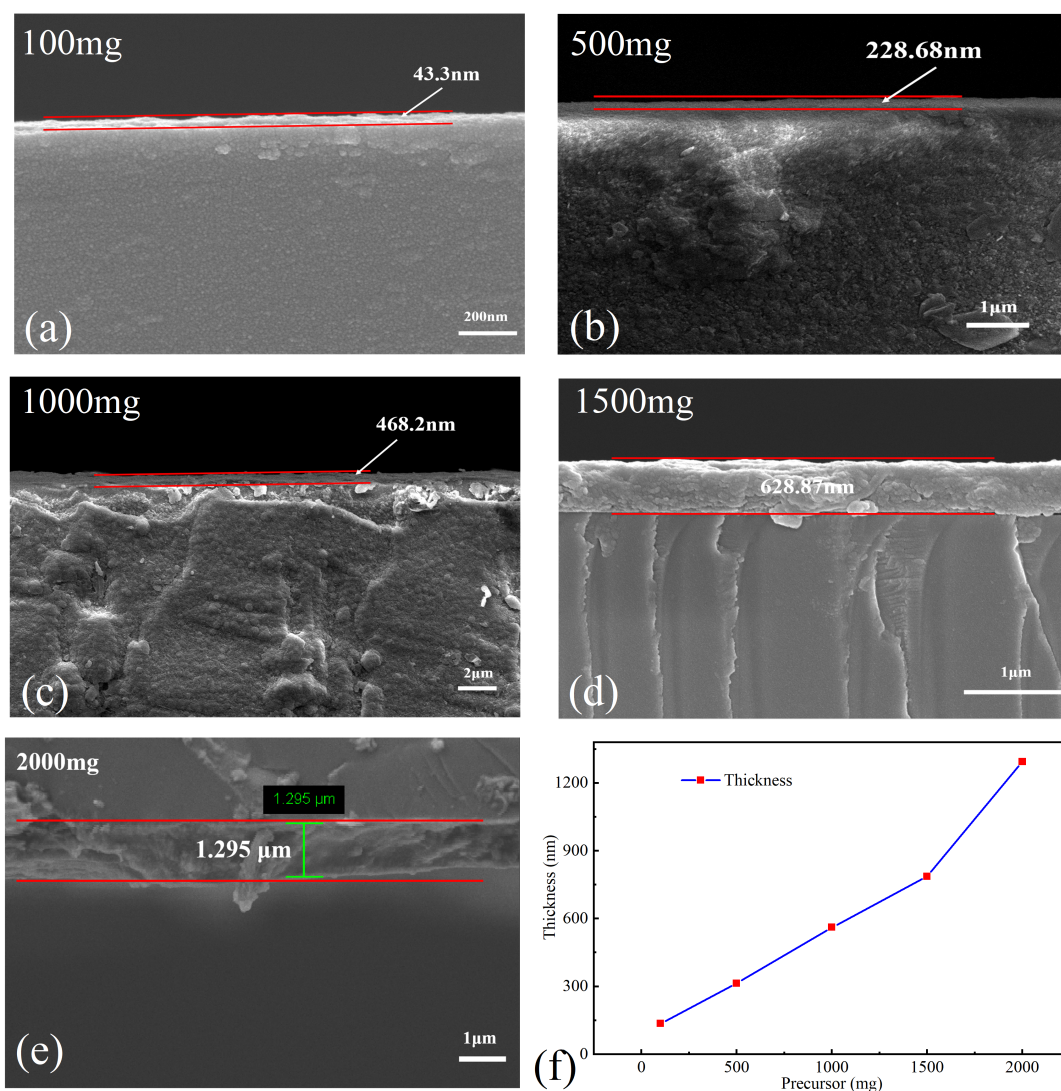


Figure 7 (a–e) Cross-sectional SEM of the h-BN film. (f) Relationship between precursor concentration and h-BN film thickness.

The cross-sectional thickness of the film was observed using SEM. As shown in Figure 7 (a–e), film growth different from the substrate was clearly observed in the cross-sectional view of the h-BN film. We have synthesized high-quality h-BN films using LPCVD. It can be seen from Figure 7 that high-quality h-BN films were epitaxially grown on the sapphire substrate and did not appear snowflake like BNH polymer [19]. As seen in Figure 7(f), the thickness of the h-BN film increased from 43.3 nm at 100 mg to 628.87 nm at 1500 mg with a linear ratio of 0.4686. However, the thickness of the h-BN film increased abruptly to 1.295  $\mu\text{m}$  when the amino-borane source mass was 2000 mg, instead of the 1023 nm obtained by linear scaling. This may be due to the fact that the amount of ammonia borane of 2000 mg at 120 degrees sublimated much more than the previous concentration, resulting in an increased concentration of ammonia borane in the CVD reactor, which also brought about faster precursor dehydrogenation and produced thicker films in the same growth time.

In our experiments, the thickness of the grown h-BN film with 2000 mg of ammonia borane observed using SEM was approximately 1.295  $\mu\text{m}$ . Heteroepitaxial growth of h-BN with a such thickness on a sapphire substrate did not lead to the peeling of h-BN from the substrate. This



phenomenon was also not observed in the other samples with different thicknesses. This is likely attributed to the formation of a thin amorphous  $\text{Al}_x\text{N}_y$  layer at the interface between h-BN and  $\text{Al}_2\text{O}_3$  when the sapphire substrate was annealed at a high temperature before h-BN growth. The nitrogen atoms from the process gas  $\text{N}_2$  replaced the oxygen atoms on the surface of the sapphire substrate, and then N–Al bonds were formed at high temperatures (greater than 1200 °C). The formation of the amorphous  $\text{Al}_x\text{N}_y$  layer reduced the lattice and thermal mismatch at the interface between h-BN and  $\text{Al}_2\text{O}_3$  and effectively released the stress at this interface [错误!未找到引用源。](#). The peak position of Raman shows that the stress between h-BN and sapphire substrate is relatively small.

If h-BN is used as a neutron detection material for radiation detection, thicker h-BN films must be needed. To date, h-BN neutron detectors have been constructed by several research groups, and the potential of h-BN in the field of neutron detection has been proven. According to Maity et al. [28], the thermal neutron absorption probability of a h-BN film with a thickness  $d$  can be expressed as

$$P(d)=1-e^{-(d/\lambda)} . \quad (1)$$

Here,  $\lambda$  represents the absorption length of thermal neutrons in h-BN. Theoretically, the  $\lambda$  value of natural h-BN materials is 238  $\mu\text{m}$  [29].

To achieve a neutron detection efficiency close to 5% for conventional neutron detectors [30], only a 10- $\mu\text{m}$ -thick h-BN film needs to be grown, and the amount of ammonia borane required is less than 20 g. Theoretically, with further optimization of the material growth process, such as growing wafer-level h-BN semiconductor materials or  $^{10}\text{B}$  enrichment, h-BN neutron detectors can achieve 100% neutron absorption.

#### 4 Conclusion

In this study, the effect of precursor amount on the thickness of h-BN films was investigated. We found that the growth rate of h-BN films increased linearly with increasing precursor concentration. We synthesized h-BN films with a thickness of 1.295  $\mu\text{m}$  by nitriding on a non-catalytic c-oriented  $\text{Al}_2\text{O}_3$  substrate using 2000 mg of monoaminoborane as a precursor. This is the thickest h-BN film grown in the reported literature so far. Due to the nitriding treatment of the substrate for 1 h prior to the growth of the h-BN film, a thin amorphous  $\text{Al}_x\text{N}_y$  layer may be formed on the sapphire surface, effectively reducing the mismatch between the sapphire and h-BN interfaces. It provides a good buffer layer for high quality h-BN growth. As a result, no h-BN peeling or cracking from the substrate was observed in our grown h-BN thin film samples of different thicknesses. If h-BN is used as a neutron-detecting material for radiation detection, thicker BN films must be grown. According to the experimental results, if a conventional neutron detector with a neutron detection efficiency close to 5% is achieved, a 10- $\mu\text{m}$ -thick h-BN film needs to be grown, and the amount of ammonia borane required is less than 20 g. This can be achieved by further optimization of the h-BN growth process. Our experiments demonstrate the potential of LPCVD for growing large-area wafer-scale h-BN for high-efficiency neutron detectors. It also provides an experimental reference for h-BN films as neutron-detecting materials.

#### Acknowledgement

This work was supported by the National Natural Science Foundation of China (Grant No. 61964001), the General Project of Jiangxi Province Key R&D Program (Grant No. 20212BBG73012), the Key Scientific Research Projects of Henan Higher Education Institutions

(Grant No. 22A490001), the State Key Laboratory of Particle Detection and Electronics (Grant No. SKLPDE-KF-2019), and the Science Foundation of Henan (No. 2022A2804).

## References

- [1] Pakdel A, Bando Y, Golberg D. Nano boron nitride flatland[J]. *Chemical Society Reviews*, 2014, 43(3): 934-959, <https://doi.org/10.1039/C3CS60260E>
- [2] Adachi S. Hexagonal Boron Nitride (h-BN)[M]//*Optical Constants of Crystalline and Amorphous Semiconductors*. Springer, Boston, MA, 1999: 127-136, [https://doi.org/10.1007/978-1-4615-5247-5\\_12](https://doi.org/10.1007/978-1-4615-5247-5_12)
- [3] Kim K K, Hsu A, Jia X, Kim S M, Shi Y, Dresselhaus M, Palacios T, Kong J. Synthesis and characterization of hexagonal boron nitride film as a dielectric layer for graphene devices[J]. *ACS nano*, 2012, 6(10): 8583-8590, <https://doi.org/10.1021/nn301675f>
- [4] Liu H, Meng J, Zhang X, Chen Y, Yin Z, Wang D, Wang Y, You J, Gao M, Jin P. High-performance deep ultraviolet photodetectors based on few-layer hexagonal boron nitride[J]. *Nanoscale*, 2018, 10(12): 5559-5565, <https://doi.org/10.1039/c7nr09438h>
- [5] Dean C R, Young A F, Meric I, Lee C, Wang L, Sorgenfrei S, Watanabe K, Taniguchi T, Kim P, Shepard K L, Hone J. Boron nitride substrates for high-quality graphene electronics[J]. *Nature nanotechnology*, 2010, 5(10): 722-726, <https://doi.org/10.1038/nnano.2010.172>
- [6] Pacile D, Meyer J C, Girit Ç Ö, Zettl A. The two-dimensional phase of boron nitride: Few-atomic-layer sheets and suspended membranes[J]. *Applied Physics Letters*, 2008, 92(13): 133107, <https://doi.org/10.1063/1.2903702>
- [7] Li X, Hao X, Zhao M, Wu Y, Yang J, Tian Y, Qian G. Exfoliation of hexagonal boron nitride by molten hydroxides[J]. *Advanced Materials*, 2013, 25(15): 2200-2204, <https://doi.org/10.1002/adma.201204031>
- [8] Lu G, Wu T, Yuan Q, Wang H, Wang H, Ding F, Xie X. Synthesis of large single-crystal hexagonal boron nitride grains on Cu-Ni alloy[J]. *Nature communications*, 2015, 6(1): 1-7, <https://doi.org/10.1038/ncomms7160>
- [9] Song L, Ci L, Lu H, Sorokin P B, Jin C, Ni J, Kvashnin A G, Kvashnin D G, Lou J, Yakobson B I, Ajayan P M. Large scale growth and characterization of atomic hexagonal boron nitride layers[J]. *Nano letters*, 2010, 10(8): 3209-3215, <https://doi.org/10.1021/nl1022139>
- [10] Song X, Li Q, Ji J, Yan Z, Gu Y, Huo C, Zou Y, Zhi C, Zeng H. A comprehensive investigation on CVD growth thermokinetics of h-BN white graphene[J]. *2D Materials*, 2016, 3(3): 035007, <https://doi.org/10.1088/2053-1583/3/3/035007>
- [11] Zhang D, Wu F, Ying Q, Gao X, Li N, Wang K, Yin Z, Cheng Y, Meng G. Thickness-tunable growth of ultra-large, continuous and high-dielectric h-BN thin films[J]. *Journal of Materials Chemistry C*, 2019, 7(7): 1871-1879, <https://doi.org/10.1039/c8tc05345f>
- [12] Ohta J, Fujioka H. Sputter synthesis of wafer-scale hexagonal boron nitride films via interface segregation[J]. *APL materials*, 2017, 5(7): 076107, <https://doi.org/10.1063/1.4995652>
- [13] Zhang W J, Matsumoto S. The effects of dc bias voltage on the crystal size and crystal quality. of cBN films[J]. *Applied Physics A*, 2000, 71(4): 469-472, <https://doi.org/10.1007/s003390000605>
- [14] Chen Y, Liang H, Abbas Q, Liu J, Shi J, Xia X, Zhang H, Du G. Growth and characterization of porous sp<sup>2</sup>-BN films with hollow spheres under hydrogen etching effect via borazane thermal CVD[J]. *Applied Surface Science*, 2018, 452: 314-321, <https://doi.org/10.1016/j.apsusc.2018.04.217>
- [15] Chen T A, Chuu C P, Tseng C C, Wen C K, Philip Wong H S, Pan S, Li R, Chao T A, Chueh W C, Zhang Y, Fu Q, Yakobson B, Chang W H, Li L J. Wafer-scale single-crystal hexagonal boron nitride monolayers on Cu (111)[J]. *Nature*, 2020, 579(7798): 219-223, <https://doi.org/10.1038/s41586-020-2009-2>
- [16] Cho H, Park S, Won D I, Kang S O, Pyo S S, Kim D I, Kim S M, Kim H C, Kim M J. Growth kinetics of white graphene (h-BN) on a planarised Ni foil surface[J]. *Scientific reports*, 2015, 5(1): 1-10, <https://doi.org/10.1038/srep11985>
- [17] Driver M S, Beatty J D, Olanipekun O, Reid K, Rath A, Voyles P M, Kelber I A. Atomic layer epitaxy of h-BN (0001)

- multilayers on Co (0001) and molecular beam epitaxy growth of graphene on h-BN (0001)/Co (0001)[J]. *Langmuir*, 2016, 32(11): 2601-2607, <https://doi.org/10.1021/acs.langmuir.5b03653>
- [18] Kim G, Jang A R, Jeong H Y, Lee Z, Kang D J, Shin H S. Growth of high-crystalline, single-layer hexagonal boron nitride on recyclable platinum foil[J]. *Nano letters*, 2013, 13(4): 1834-1839, <https://doi.org/10.1021/nl400559s>
- [19] Chen Y, Liang H, Xia X, et al. Growth temperature impact on film quality of hBN grown on Al<sub>2</sub>O<sub>3</sub> using non-catalyzed borazane CVD[J]. *Journal of Materials Science: Materials in Electronics*, 2017, 28(19): 14341-14347. <https://doi.org/10.1007/s10854-017-7294-7>
- [20] Kim K K, Kim S M, Lee Y H. A new horizon for hexagonal boron nitride film[J]. *Journal of the Korean physical society*, 2014, 64(10): 1605-1616, <https://doi.org/10.3938/jkps.64.1605>
- [21] Frueh S, Kellett R, Mallery C, Molter T, Willis W S, King'ondeu C, Suib S L. Pyrolytic decomposition of ammonia borane to boron nitride[J]. *Inorganic chemistry*, 2011, 50(3): 783-792, <https://doi.org/10.1021/ic101020k>
- [22] Zhong B, Zhang T, Huang X X, Wen G W, Chen J W, Wang C J, Huang Y D. Fabrication and Raman scattering behavior of novel turbostratic BN thin films[J]. *Materials Letters*, 2015, 151: 130-133, <https://doi.org/10.1016/j.matlet.2015.03.059>
- [23] Li X, Sundaram S, El Gmili Y, Ayari T, Puybaret R, Patriarche G, Voss P L, Salvestrini J P, Ougazzaden A. Large-area two-dimensional layered hexagonal boron nitride grown on sapphire by metalorganic vapor phase epitaxy[J]. *Crystal Growth & Design*, 2016, 16(6): 3409-3415, <https://doi.org/10.1021/acs.cgd.6b00398>
- [24] Ishigami M, Aloni S, Zettl A. Properties of boron nitride nanotubes[C]//AIP conference proceedings. American Institute of Physics, 2003, 696(1): 94-99, <https://doi.org/10.1063/1.1639682>
- [25] Maity A, Doan T C, Li J, Jiang H X. Realization of highly efficient hexagonal boron nitride neutron detectors[J]. *Applied physics letters*, 2016, 109(7): 072101, <https://doi.org/10.1063/1.4960522>
- [26] Chubarov M, Högberg H, Henry A, et al. Challenge in determining the crystal structure of epitaxial 0001 oriented sp<sup>2</sup>-BN films[J]. *Journal of Vacuum Science & Technology A: Vacuum, Surfaces, and Films*, 2018, 36(3): 030801. <https://doi.org/10.1116/1.5024314>
- [27] Yamada H, Inotsume S, Kumagai N, Yamada T, Shimizu M. Chemical Vapor Deposition Growth of BN Thin Films Using B<sub>2</sub>H<sub>6</sub> and NH<sub>3</sub>[J]. *physica status solidi (b)*, 2020, 257(2): 1900318. <https://doi.org/10.1002/pssb.201900318>
- [28] Maity A, Doan T C, Li J, Jiang H X. Realization of highly efficient hexagonal boron nitride neutron detectors[J]. *Applied physics letters*, 2016, 109(7): 072101, <https://doi.org/10.1063/1.4960522>.
- [29] Li J, Dahal R, Majety S, Lin J Y, Jiang H X. Hexagonal boron nitride epitaxial layers as neutron detector materials[J]. *Nuclear instruments and methods in physics research section a: accelerators, spectrometers, detectors and associated equipment*, 2011, 654(1): 417-420, <https://doi.org/10.1016/j.nima.2011.07.040>
- [30] Jiang Y, Wu J, Yin Y, et al. Improving thermal-neutron detection efficiency of silicon neutron detectors using the combined layers of 10B<sub>4</sub>C on 6LiF[J]. *Nuclear Instruments and Methods in Physics Research Section A: Accelerators, Spectrometers, Detectors and Associated Equipment*, 2019, 932: 50-55. <https://doi.org/10.1016/j.nima.2019.04.051>